

Fluorescence Assay for the Binding of Ribonuclease A to the Ribonuclease Inhibitor Protein

Richele L. Abel,* Marcia C. Haigis,* Chiwook Park,*¹ and Ronald T. Raines*^{†,2}

*Department of Biochemistry and †Department of Chemistry, University of Wisconsin at Madison, Madison, Wisconsin 53706

Received December 7, 2001; published online June 5, 2002

Ribonuclease A (RNase A) and the ribonuclease inhibitor protein (RI) form one of the tightest known protein–protein complexes. RNase A variants and homologues, such as G88R RNase A, that retain ribonucleolytic activity in the presence of RI are toxic to cancer cells. Herein, a new and facile assay is described for measuring the equilibrium dissociation constant (K_d) and dissociation rate constant (k_d) for complexes of RI and RNase A. This assay is based on the decrease in fluorescence intensity that occurs when a fluorescein-labeled RNase A binds to RI. To allow time for equilibration, the assay is most readily applied to those complexes with K_d values in the nanomolar range or higher. Using this assay, the value of K_d for the complex of RI with fluorescein-labeled G88R RNase A was determined to be 0.55 ± 0.03 nM. In addition, the value of K_d was determined for the complex of RI with unlabeled G88R RNase A to be 0.57 ± 0.05 nM by using a competition assay with fluorescein-labeled G88R RNase A. Finally, the value of k_d for the complex of RI with fluorescein-labeled G88R RNase A was determined to be $(7.5 \pm 0.4) \times 10^{-3} \text{ s}^{-1}$ by monitoring the increase in fluorescence intensity upon dissociation. This assay can be used to characterize complexes of RI with a wide variety of RNase A variants and homologues, including those with cytotoxic activity. © 2002 Elsevier Science (USA)

Key Words: competition assay; equilibrium dissociation constant; fluorescence spectroscopy; protein–protein interaction; ribonuclease A; ribonuclease inhibitor.

Ribonuclease A (RNase A,³ EC 3.1.27.5) and its cytosolic protein inhibitor, ribonuclease inhibitor (RI), have an extraordinary affinity for one another. RNase A is a 13.7-kDa enzyme that is secreted from the exocrine cells of the bovine pancreas (1, 2). This enzyme is an efficient catalyst, degrading RNA with a k_{cat}/K_M value that can exceed $10^9 \text{ M}^{-1} \text{ s}^{-1}$ (3). RI is a 50-kDa protein that is found in the cytosol of all mammalian cells tested (4–6). The unusual horseshoe structure of RI evolved by the rapid duplication of exons encoding 57-residue modules (7).

RI binds to RNase A in a 1:1 stoichiometry, burying 2550 \AA^2 of surface area (8). A structure of the crystal-line complex is shown in Fig. 1. RI inhibits the ribonucleolytic activity of RNase A and other proteins in the RNase A superfamily, including RNase 1 (9, 10), RNase 2 (9, 11), RNase 4 (9), and angiogenin (12, 13). Reported K_d values for the RI · RNase A complex are 44 fM with human RI (13) and 59 fM with porcine RI (14), making the RI–RNase A interaction one of the strongest known. The RI · angiogenin complex is even tighter, with a K_d value of 0.71 fM (13). Still, the biological function of RI, as well as the biological imperative for these tight interactions, remains unclear. Presumably, because RI is located in the cytosol and members of the RNase A superfamily are secreted from cells, these two proteins are unlikely to encounter one another. Hence, the role of RI could be to protect the cell from secreted ribonucleases that happen to enter the cytosol (15) or to regulate angiogenin (16), which has been shown to play a role in the development of new blood vessels (17–19).

¹ Current address: Department of Molecular and Cell Biology, University of California, Berkeley, 229 Stanley Hall, Berkeley, CA 94720.

² To whom correspondence should be addressed at the Department of Biochemistry, University of Wisconsin at Madison, 433 Babcock Drive, Madison, WI 53706-1544. Fax: (608) 262-3453. E-mail: raines@biochem.wisc.edu.

³ Abbreviations used: DTT, dithiothreitol; fluorescein–G88R RNase A, G88R RNase A covalently labeled with fluorescein on residue 19; fluorescein–RNase A, RNase A covalently labeled with fluorescein on residue 19; 5'-IAF, 5'-iodoacetamidofluorescein; PBS, phosphate-buffered saline; PDB, protein data bank; RNase A, bovine pancreatic ribonuclease A; RI, ribonuclease inhibitor; TCEP, tris-(carboxyethyl)phosphine hydrochloride; MALDI-TOF, matrix-assisted laser desorption/ionization time-of-flight; TFA, trifluoroacetic acid.

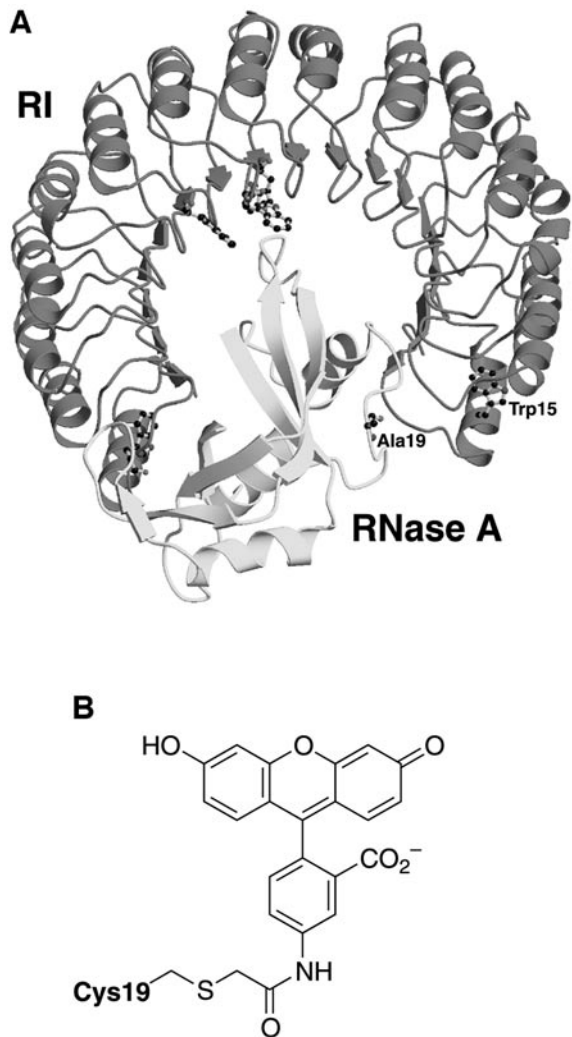


FIG. 1. (A) Structure of the crystalline porcine RI · RNase A complex [PDB entry 1DFJ (8)]. The five tryptophan residues in RI (Trp15, Trp257, Trp259, Trp314, and Trp434) and Ala19 of RNase A are indicated. (B) Structure of the fluorescein moiety attached to residue 19 of fluorescein-RNase A and fluorescein-G88R RNase A.

Evaluating the affinity of RI for RNase A variants or homologues is of substantial importance. The ability of a variant or homologue to retain ribonucleolytic activity in the presence of RI correlates with its toxicity for cancer cells (20–22). Hence, there is much effort to create active variants that have even lower affinity for RI (23). For example, replacing Gly88 of RNase A with an arginine residue reduces its affinity for RI and makes it cytotoxic (20). The inspiration for these efforts is a homologue from the Northern leopard frog (*Rana pipiens*) called Onconase (24). Onconase is a potent cytotoxin that is in Phase III clinical trials for the treatment of malignant mesothelioma. The K_d for the RI · Onconase complex has not yet been determined, but has been estimated to be $\geq 10^{-6}$ M (25).

Determining the affinity of RI for RNase A and its variants has not been trivial. Vallee and co-workers first

determined the value of K_d for the complexes of human RI with both RNase A and angiogenin by measuring the association and dissociation rate constants (13). Their assays were based on the increase in the fluorescence of Trp89 of angiogenin upon its binding to RI (26). Hofsteenge and co-workers determined the value of K_i for the porcine RI · RNase A complex by measuring the decrease in ribonucleolytic activity as additional RI was added to a solution containing RNA (14). Determining the K_i of the RI · RNase A complex in their manner is difficult for the many members of the RNase A superfamily, such as Onconase and angiogenin, that have low ribonucleolytic activity.

Here, we describe a facile assay for characterizing the RI–RNase A interaction. This assay uses an RNase A variant labeled at a specific residue with fluorescein. We find that binding to RI decreases the fluorescence intensity of the variant. We use this finding to evaluate the affinity of RI for labeled G88R RNase A directly, as well as that for unlabeled G88R RNase A in a competition assay. Finally, we use the competition assay to determine the dissociation rate constant for the complex of RI with fluorescein-labeled G88R RNase A.

MATERIALS AND METHODS

Materials

Escherichia coli strain BL21 (DE3) was from Novagen (Madison, WI), and strain TOPP 3 was from Stratagene (La Jolla, CA). 5'-Iodoacetamidofluorescein (5'-IAF) was from Molecular Probes (Eugene, OR). All other reagents were from Sigma Chemical (St. Louis, MO).

An FPLC Hiload 26/60 Superdex 75 gel-filtration column, mono-S HR10/10 cation-exchange column, and PD-10 desalting columns were from Amersham Pharmacia Biotech (Piscataway, NJ). An HPLC system equipped with an auto injector and a photo diode array detector was from Waters (Milford, MA).

Phosphate-buffered saline (PBS; pH 7.3) contained (in 1.00 liter) KCl (0.20 g), KH_2PO_4 (0.20 g), NaCl (8.0 g), and $\text{Na}_2\text{HPO}_4 \cdot 7\text{H}_2\text{O}$ (2.16 g). All other chemical reagents were of commercial reagent grade or better and were used without further purification.

Analytical Instruments

Fluorescence measurements were made at room temperature ($23 \pm 2^\circ\text{C}$) on a QuantaMaster1 photon-counting fluorometer from Photon Technology International (South Brunswick, NJ) equipped with sample stirring. Fluorescence grade quartz or glass cuvettes (1.0-cm pathlength, 3.0-ml volume) from Starna Cells were used with the fluorescence spectrophotometer. Solution concentrations of RI and RNase A variants were determined by measuring UV absorbance with a Cary Model 50 spectrophotometer from Varian (Sugar Land, TX). MALDI-TOF mass spectra were obtained with a Bruker Biflex III matrix-assisted laser desorp-

tion/ionization time-of-flight instrument at the University of Wisconsin Biotechnology Center. The programs DELTAGRAPH (DeltaPoint, Monterey, CA) and SIGMAPLOT (SPSS Science, Chicago, IL) were used to analyze the data presented herein.

Preparation of Ribonuclease Inhibitor

Porcine RI was prepared according to a method described previously (27). The concentration of RI was determined by using $\epsilon = 0.88 \text{ ml mg}^{-1} \text{ cm}^{-1}$ at 280 nm (28). RI was stored at 4°C in PBS containing dithiothreitol (DTT; 10 mM), which prevents oxidation of its 32 cysteine residues.

Preparation of Fluorescein-Labeled Ribonuclease A

Fluorescein-labeled RNase A (fluorescein–RNase A), which has a thioether linkage between residue 19 and a fluorescein moiety (Fig. 1B), was prepared essentially as described previously (29). Briefly, RNase A and its G88R variant were labeled at one specific residue by using a variant in which Ala19 was replaced with a cysteine residue (29, 30). Ala19 was chosen because it is in a solvent-exposed loop that is not in the RI · RNase A interface (8). A19C RNase A and A19C/G88R RNase A were prepared according to methods described previously for other RNase A variants (31, 20). During their folding and purification, proteins were kept under Ar(g) to prevent oxidation of Cys19. After purification, the thiol of Cys19 was protected from inadvertent air oxidation by reaction with 5,5'-dithiobis(2-nitrobenzoic acid) (Sigma Chemical) (32, 33). The protected protein was purified from unprotected protein by cation-exchange chromatography. The pH of the protein solution was raised to ~8 by the addition of Tris (2 M), and the protein was deprotected by the addition of a 3-fold molar excess of either DTT or tris-(carboxyethyl)phosphine hydrochloride (Sigma Chemical). Deprotected proteins were reacted quickly with a 40-fold molar excess of 5'-IAF (Molecular Probes). Unreacted 5'-IAF was removed from the labeled protein by chromatography on a PD-10 desalting column.

Purification of Fluorescein-Labeled Ribonuclease A

Proteins deprotected with DTT were incompletely labeled by 5'-IAF. Fluorescein–RNase A was purified by reversed-phase HPLC with a Varian C-4 semipreparatory column. Protein was eluted with an isocratic gradient of aqueous acetonitrile (28% v/v) containing trifluoroacetic acid (TFA; 0.1% v/v) at a flow rate of 3.5 ml/min. Purified fluorescein–RNase A was obtained by collecting those fractions with absorbance at both 277 and 495 nm. HPLC-purified proteins were dialyzed extensively against PBS. Proteins deprotected with TCEP were >95% labeled and did not require additional purification. The molecular mass and purity of labeled proteins were verified with MALDI-TOF mass

spectrometry. The concentration of labeled RNase A was determined by using $\epsilon = 0.72 \text{ ml mg}^{-1} \text{ cm}^{-1}$ at 277.5 nm (34) after correction for the absorbance of the fluorescein moiety by using an equation provided by Molecular Probes: $A_{277.5 \text{ nm}}^{\text{protein}} = A_{277.5 \text{ nm}} - (A_{494 \text{ nm}}/5)$.

Preparation of Angiogenin

Human angiogenin was prepared according to a method described previously (35). The concentration of angiogenin was determined by using $\epsilon = 0.85 \text{ ml mg}^{-1} \text{ cm}^{-1}$ at 278 nm (36).

Binding Assay

Fluorescence spectroscopy was used to monitor the binding of RI to either fluorescein–RNase A or fluorescein–G88R RNase A. Briefly, as increasing amounts of RI were added, the fluorescence intensity decreased. RI was added until the fluorescence stopped decreasing, which presumably indicated that the fluorescein–RNase A was bound completely by RI.

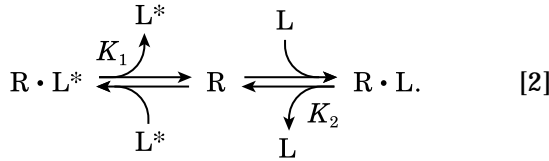
Specifically, fluorescence intensity was measured in PBS containing DTT (5 mM) and fluorescein–RNase A (18.4 nM) or fluorescein–G88R RNase A (0.8 nM). The fluorescein moiety was excited at 491 nm, and its emission was monitored at 511 nm. The initial fluorescence intensity was determined once the fluorescence stabilized, that is, after at least 30 min. Aliquots of RI (final concentration 1.8–20 nM for fluorescein–RNase A, 20 pM–90.5 nM for fluorescein–G88R RNase A) were added, and the fluorescence was recorded after each addition. The fraction of bound fluorescein-labeled RNase A (f) was calculated by determining the decrease in fluorescence intensity of the sample compared to the decrease when fluorescein-labeled RNase A was bound completely. The data were fitted to Eq. [1] to determine the value of K_d .⁴

$$f = \frac{[\text{RI}]}{[\text{RI}] + K_d} \quad [1]$$

Competition Assay

In a competition assay, there is a mixture of two different ligands (L and L*) that each can bind to the same receptor (R) at a common site (37). The relevant equilibria are depicted in Eq. [2]:

⁴ Using Eq. [1] assumes that $[\text{RI}] = [\text{RI}]_{\text{total}}$. This condition is ensured if the value of K_d is much greater than the assay concentration of fluorescein-labeled ligand, which is likely to be true for a cytotoxic ribonuclease. If not, then a variation of Eq. [1] in ref. 20 should be used instead. For fluorescein–G88R RNase A, the values of K_d determined in these two ways do not differ significantly.



Here, R represents RI, L^* represents fluorescein-G88R RNase A, and L represents unlabeled G88R RNase A. The equilibrium dissociation constant K_1 is for the RI · fluorescein-G88R RNase A complex, and the equilibrium dissociation constant K_2 is for the RI · G88R RNase A complex. This method and Eq. [3] can be used to determine the value of K_1 or K_2 , assuming that either one is known:

$$\begin{aligned}
 & R \cdot L^* \\
 & \left(L_T^* + R_T + \frac{K_1}{K_2} (L_T - R_T) \right) \\
 & - \sqrt{\left(L_T^* + R_T + \frac{K_1}{K_2} (L_T - R_T) \right)^2 - 4 \left(1 - \frac{K_1}{K_2} \right) L_T^* R_T} \\
 & = \frac{\quad}{2 \left(1 - \frac{K_1}{K_2} \right)}.
 \end{aligned} \quad [3]$$

In Eq. [3], R_T is the total concentration of RI, which is constant. L_T^* is the total concentration of fluorescein-G88R RNase A, which is constant. L_T is the total concentration of unlabeled G88R RNase A added, which is a known variable. The value of one equilibrium dissociation constant must be known, and the value of the other is determined as Eq. [3] is fitted to the data. $R \cdot L^*$ is the concentration of the RI · fluorescein-G88R RNase A complex, which is apparent from the decrease in the fluorescence of fluorescein-G88R RNase A upon addition of RI. As unlabeled RNase A is added to the cuvette, it competes for RI, leaving more fluorescein-G88R RNase A unbound.

Specifically, the value of K_d for the RI · G88R RNase A complex was measured by using the known K_d value of the RI · fluorescein-G88R RNase A complex. The assay was done in PBS containing fluorescein-G88R RNase A (50 nM) and DTT (5 mM). First, the initial fluorescence intensity was measured. Next, RI was added (to 50 nM), and the fluorescence was measured after several minutes of equilibration. Then, aliquots of unlabeled G88R RNase A (final concentration 1.0 nM–0.50 μ M) were added, and the fluorescence was measured after each addition. The concentration of the RI · fluorescein-G88R RNase A complex was determined by comparing the fluorescence to that when fluorescein-G88R RNase A was completely free or completely bound by RI.

Kinetic Assay

The dissociation rate constant for the RI · fluorescein-G88R RNase A complex was determined by using

fluorescence spectroscopy. Briefly, an equimolar solution of RI and fluorescein-G88R RNase A was allowed to reach equilibrium. The concentrations of RI and fluorescein-G88R RNase A were well above the K_d value for the RI · fluorescein-G88R RNase A complex. A molar excess of human angiogenin, which has the highest known affinity for RI (13), was then added to the cuvette to scavenge free RI (13, 38–40). The increase in fluorescence as the RI · fluorescein-G88R RNase A complex dissociated irreversibly was monitored over time.

Specifically, fluorescein-G88R RNase A (0.10 μ M) was added to PBS containing DTT (5 mM), and the initial fluorescence was recorded. RI was then added (to 0.10 μ M) and the fluorescence decreased, indicating that the RI · fluorescein-G88R RNase A complex had formed. Angiogenin was added (to 0.23 μ M), and the fluorescence was recorded. The data were fitted to a first-order exponential equation [i.e., fluorescence = fluorescence _{$t=0$} + (fluorescence _{$t=\infty$} - fluorescence _{$t=0$}) (1 - e^{- $k_d t$})] to determine the value of the dissociation rate constant, k_d .

Derivation of Equation for Competition Assay

The purpose of Eq. [3] is to enable the determination of the value of K_d for a complex of a receptor and ligand in a competition assay. In this competition assay, a ligand labeled with fluorescein (L^*) and an unlabeled ligand (L) are competing for binding to the same site on the receptor (R), as in Eq. [2]. The equilibrium dissociation constants for the $R \cdot L^*$ complex and the $R \cdot L$ complex, K_1 and K_2 , are defined in Eqs. [4] and [5], respectively:

$$K_1 = \frac{R \times L^*}{R \cdot L^*}, \quad [4]$$

$$K_2 = \frac{R \times L}{R \cdot L}. \quad [5]$$

Because the values of L^* , L, and $R \cdot L$ are unknown, Eqs. [4] and [5] are more useful in terms of L_T^* , L_T , and R_T , which are known and related to L^* , L, and $R \cdot L$ by mass conservation:

$$L^* = L_T^* - R \cdot L^*, \quad [6]$$

$$L = L_T - R_T + R \cdot L^*, \quad [7]$$

$$R \cdot L = R_T - R \cdot L^*. \quad [8]$$

The derivation of Eq. [7] assumes that the receptor is bound completely under the conditions of the assay (that

is, $R = 0$ such that $R_T = R \cdot L^* + R \cdot L$, as in Eq. [8]). Substituting Eqs. [6–8] into Eqs. [4] and [5] yields

$$K_1 = \frac{R(L_T^* - R \cdot L^*)}{R \cdot L^*}, \quad [9]$$

$$K_2 = \frac{R(L_T - R_T + R \cdot L^*)}{(R_T - R \cdot L^*)}. \quad [10]$$

Solving for R in Eqs. [9] and [10] yields

$$R = \frac{K_1 \times R \cdot L^*}{L_T^* - R \cdot L^*} \quad [11]$$

and

$$R = \frac{K_2(R_T - R \cdot L^*)}{L_T - R_T + R \cdot L^*}. \quad [12]$$

Equating Eqs. [11] and [12] yields

$$\frac{K_1 \times R \cdot L^*}{L_T^* - R \cdot L^*} = \frac{K_2(R_T - R \cdot L^*)}{L_T - R_T + R \cdot L^*}. \quad [13]$$

Rearranging Eq. [13] yields

$$\begin{aligned} \frac{K_1}{K_2} (R \cdot L^*)^2 + \frac{K_1}{K_2} (R \cdot L^*)(L_T - R_T) \\ = (R \cdot L^*)^2 - (R \cdot L^*)(L_T^* + R_T) + L_T^* R_T \end{aligned} \quad [14]$$

and

$$\begin{aligned} (R \cdot L^*)^2 \left(1 - \frac{K_1}{K_2}\right) - (R \cdot L^*) \\ \times \left(L_T^* + R_T + \frac{K_1}{K_2} (L_T - R_T)\right) + L_T^* R_T = 0. \end{aligned} \quad [15]$$

Equation [15] is a quadratic equation, which is solved for the meaningful value of $R \cdot L^*$ in Eq. [3].

RESULTS

Purification of Fluorescein-Labeled RNase A

The purification of fluorescein–RNase A from unlabeled RNase A was achieved by using reversed-phase HPLC as shown in Fig. 2. The mass of the product, fluorescein–RNase A, was 14.1 kDa (expected: 14.1 kDa). No unlabeled A19C RNase A (expected: 13.7 kDa) was detected in the purified sample by MALDI-TOF mass spectrometry.

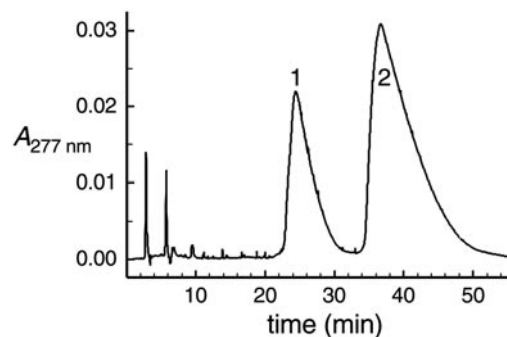


FIG. 2. Chromatogram of purification of fluorescein–RNase A by reversed-phase HPLC. Proteins were eluted from a C-4 column with aqueous acetonitrile (28% v/v) containing TFA (0.1% v/v) at a flow rate of 3.5 ml/min. Protein was detected by monitoring absorbance at 277 nm. Peak 1 is unlabeled A19C RNase A; peak 2 is fluorescein–RNase A.

Decrease in Fluorescence of Fluorescein-Labeled Ribonuclease A

The fluorescence intensity of fluorescein–RNase A decreases by nearly 20% upon addition of RI, as shown in Fig. 3A. These raw data were used to calculate the fraction of bound fluorescein–RNase A. The concentrations used to generate these data were well above the known K_d for the RI · RNase A complex. Hence, a linear relationship was expected between the concentration of RI · fluorescein–RNase A complex and that of added RI. A linear relationship was indeed observed, as shown in Fig. 3B. Linear regression analysis of these data gives $R^2 = 0.992$. This value near unity verifies the high precision of this method for determining the concentration of the RI · fluorescein–RNase A complex.

Binding Assay with Fluorescein-Labeled G88R Ribonuclease A

Fluorescein–G88R RNase A, which was prepared in the same manner as fluorescein–RNase A, was titrated with RI. The data from multiple assays were combined and fitted with Eq. [1], as shown in Fig. 4. The RI · fluorescein–G88R RNase A complex was determined to have $K_d = 0.55 \pm 0.03$ nM.

Competition Assay with G88R Ribonuclease A

The competition assay was used to determine the value of K_d for the RI · G88R RNase A complex, using the known value of K_d for the RI · fluorescein–G88R RNase A complex (Fig. 4). The concentration of the RI · fluorescein–G88R RNase A complex was determined and plotted against the concentration of G88R RNase A (Fig. 5) and fitted to Eq. [3]. Assuming that the value of K_d for the RI · fluorescein–G88R RNase A complex was 0.55 nM, then the K_d of the RI · fluorescein–RNase A complex was determined from Eq. [3] to be 0.57 ± 0.05 nM.

Kinetic Assay with Fluorescein-Labeled G88R Ribonuclease A

The kinetic assay was used to determine the value of the dissociation rate constant, k_d , for the RI · fluorescein-G88R RNase A complex. Data were fitted to a first-order exponential equation, and data from one assay are shown in Fig. 6. The RI · fluorescein-G88R RNase A complex was determined to have $k_d = (7.5 \pm 0.4) \times 10^{-3} \text{ s}^{-1}$, which is the mean \pm SE from multiple assays.

DISCUSSION

We have developed a new method for determining the fraction of an RNase A variant that is bound to RI

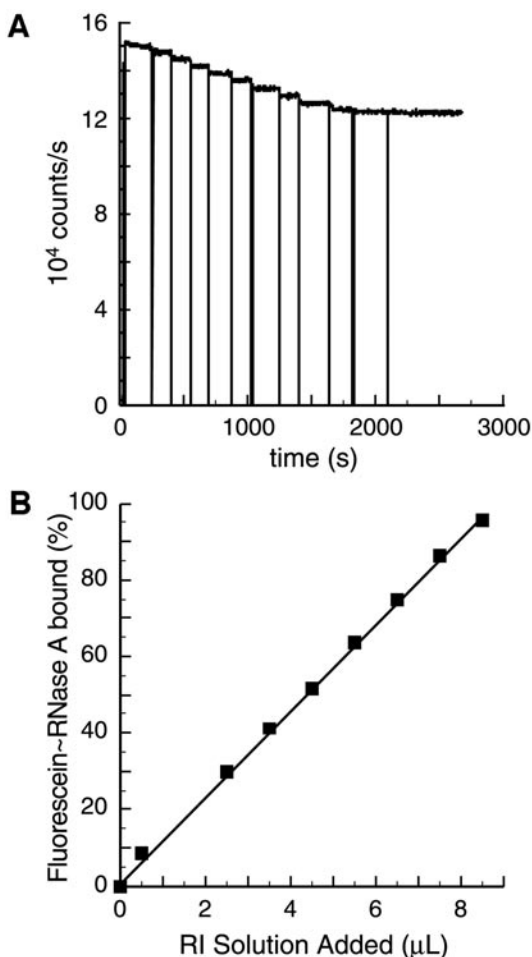


FIG. 3. (A) Raw fluorescence intensity data for the binding of fluorescein-RNase A to RI. The fluorescence of fluorescein-RNase A (18.4 nM) in PBS containing DTT (5 mM) was measured by its excitation at 491 nm and emission at 511 nm. RI was added in 0.5- to 1- μl aliquots, each μl increasing the concentration of RI by 1.8 nM, until subsequent addition no longer resulted in a decrease in fluorescence. The final intensity was 81.6% of the initial intensity. (B) Transformed data for binding of fluorescein-RNase A by RI. Fluorescence intensities from A were used to calculate the fraction of fluorescein-RNase A bound to RI at each RI concentration. Linear regression analysis yielded $R^2 = 0.992$.

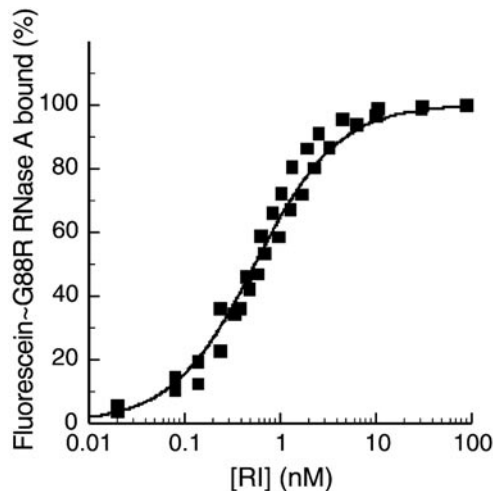


FIG. 4. Titration of fluorescein-G88R RNase A with RI. Increasing amounts of RI (20 pM–90.5 nM) were added to fluorescein-G88R RNase A (0.80 nM) in PBS containing DTT (5 mM). The plot shows data collected from two independent titrations. The data were fitted to Eq. [1], and the K_d value for the RI · fluorescein-G88R RNase A complex was determined to be 0.55 ± 0.03 nM.

in an assay mixture. This method is based on the nearly 20% decrease in fluorescence intensity that occurs when RNase A that is labeled with fluorescein at residue 19 binds to RI (Fig. 3A). The chemical basis for the decrease in fluorescence is unknown. A likely explanation is that the pK_a of the fluorescein moiety increases slightly upon binding to RI, as has been observed for the binding of fluorescein-labeled S peptide to S protein (41, 42).⁵

First, we demonstrated the ability of this method to reveal the amount of fluorescein-RNase A that is bound in an RI · fluorescein-RNase A complex (Fig. 3B). In this experiment, the concentrations of RI and fluorescein-RNase A were well above the K_d value for the complex. Hence, as additional RI was added to the sample, it was bound completely by fluorescein-RNase A, decreasing the fluorescence of the fluorescein moiety. Fluorescence continued to decrease in a linear manner with each subsequent addition of RI.

Next, we used the decrease in fluorescence to determine the value of K_d for the RI · fluorescein-G88R RNase A complex. This direct titration gave a value of $K_d = 0.55 \pm 0.03$ nM (Fig. 4). This value is in gratifying agreement with the value of $K_i = 0.41$ nM determined previously by monitoring the decrease in the ribonucleolytic activity of G88R RNase A as additional human RI was added to a solution containing RNA (20).

⁵ Another spectroscopic consequence of the binding of fluorescein-RNase A could be the quenching of the fluorescence of one or more of the five tryptophan residues of RI (Fig. 1A). Trp15 of porcine RI is most proximal to residue 19 of RNase A, with a C α -C α distance of 30.6 Å (8).

Then, we used a competition assay and the known K_d value of the RI · fluorescein–G88R RNase A complex to assess the affinity of unlabeled G88R RNase A for RI. This competition assay gave a value of $K_d = 0.57 \pm 0.05$ nM for the RI · G88R RNase A complex (Fig. 5). The similarity of the K_d values for the RI · fluorescein–G88R RNase A complex and the RI · G88R RNase A complex suggests that the fluorescein moiety of fluorescein–G88R RNase A has little effect on its affinity for RI.

Finally, we demonstrated how the dissociation rate constant of the RI · fluorescein–G88R RNase A complex can be measured directly. This assay yielded a dissociation rate constant of $k_d = (7.5 \pm 0.4) \times 10^{-3} \text{ s}^{-1}$ (Fig. 6). From this value and the value of $K_d = 0.55 \pm 0.03$ nM, the value of the association rate constant was calculated to be $k_a = k_d/K_d = (1.4 \pm 0.2) \times 10^7 \text{ M}^{-1} \text{ s}^{-1}$. Comparing our values to those reported previously for the complex of human RI with wild-type RNase A [$k_d = 1.5 \times 10^{-5} \text{ s}^{-1}$ (5), $1.2 \times 10^{-5} \text{ s}^{-1}$ (38, 40); and $k_a = 3.4 \times 10^8 \text{ M}^{-1} \text{ s}^{-1}$ (5), $3.8 \times 10^8 \text{ M}^{-1} \text{ s}^{-1}$ (38), $2.8 \times 10^8 \text{ M}^{-1} \text{ s}^{-1}$ (40)] suggests that replacing Gly88 of RNase A with an arginine residue has a greater effect on the rate of dissociation of the RI · RNase A complex than on the rate of association of RI and RNase A.

Limitations of Assay

The assays described herein do have a practical limitation. Only complexes of RI with RNase A that have values of K_d in the nM range or higher are amenable to study without long incubation times. This limitation arises because tighter complexes require a long time to

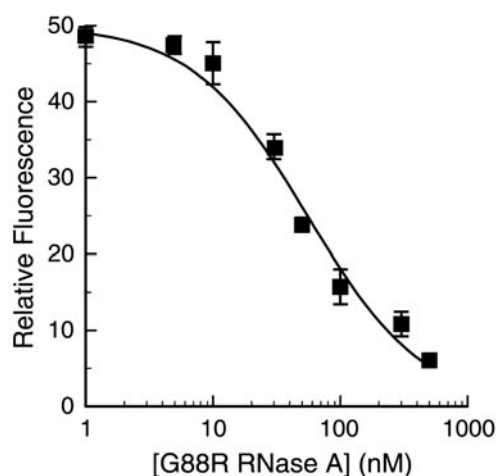


FIG. 5. Competition assay for binding of G88R RNase A to RI. Assays contained fluorescein–G88R RNase A (50 nM), RI (50 nM), and G88R RNase A (1.0 nM–0.50 μM) in PBS containing DTT (5 mM). The concentration of bound fluorescein–G88R RNase A was calculated as described in the text. The data were fitted to Eq. [3], and the K_d value for the RI · G88R RNase A complex was determined to be 0.57 ± 0.05 nM.

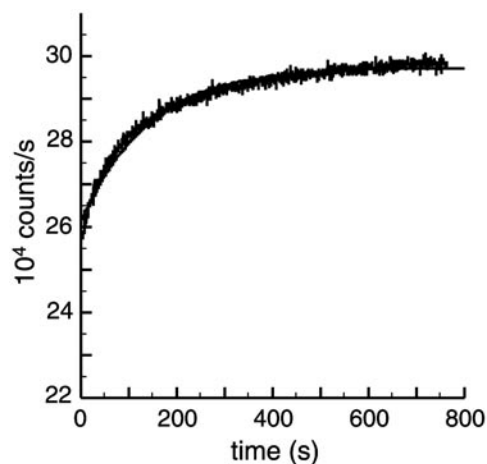


FIG. 6. Raw fluorescence intensity data for the dissociation of the RI · fluorescein–G88R RNase A complex. The fluorescence of the fluorescein–G88R RNase A complex (0.10 μM) in PBS containing DTT (5 mM) was measured by its excitation at 491 nm and emission at 511 nm. At $t = 0$, angiogenin (0.23 μM) was added to scavenge free RI. The dissociation of the RI · fluorescein–G88R RNase A complex is irreversible, and the fluorescence increases. The k_d value for the RI · fluorescein–G88R RNase A complex was determined to be $7.5 \pm 0.4 \text{ s}^{-1}$.

reach equilibrium. For example, the RI · RNase A complex has a half-life of 13 h, and the RI · angiogenin complex has a half-life of approximately 60 days (13).

Conclusions

The new assay described herein is a convenient means to characterize the thermodynamics and kinetics of the interaction of RI with RNase A variants and homologues. We expect that the competition assay, which requires labeling only one protein, will be of particular use to workers interested in creating new variants that evade RI and are thus endowed with cytotoxic activity. Such variants have potential as cancer chemotherapeutics (23).

ACKNOWLEDGMENTS

We thank B. D. Smith for the generous gift of A19C/G88R RNase A. R.L.A. was supported by Molecular Biophysics Training Grant GM08293 (NIH). This work was supported by grants GM44783 and CA73808 (NIH).

REFERENCES

1. Cuchillo, C. M., Vilanova, M., and Nogués, M. V. (1997) *in* Ribonucleases: Structures and Functions (D'Alessio, G., and Riordan, J. F., Eds.), pp. 271–304, Academic Press, New York.
2. Raines, R. T. (1998) Ribonuclease A. *Chem. Rev.* **98**, 1045–1065.
3. Park, C., and Raines, R. T. (2001) Quantitative analysis of the effect of salt concentration on enzymatic catalysis. *J. Am. Chem. Soc.* **123**, 11472–11479.
4. Kobe, B., and Deisenhofer, J. (1994) The leucine-rich repeat: A versatile binding motif. *Trends Biochem. Sci.* **19**, 415–421.

5. Hofsteenge, J. (1997) in *Ribonucleases: Structures and Functions* (D'Alessio, G., and Riordan, J. F., Eds.), pp. 621–658, Academic Press, New York.
6. Shapiro, R. (2001) Cytoplasmic ribonuclease inhibitor. *Methods Enzymol.* **341**, 611–628.
7. Haigis, M. C., Haag, E. S., and Raines, R. T. (2002) Evolution of ribonuclease inhibitor by gene duplication. *Mol. Biol. Evol.* **19**, 960–964.
8. Kobe, B., and Deisenhofer, J. (1996) Mechanism of ribonuclease inhibition by ribonuclease inhibitor protein based on the crystal structure of its complex with ribonuclease A. *J. Mol. Biol.* **264**, 1028–1043.
9. Sorrentino, S., Glitz, D. G., Hamann, K. J., Loegering, D. A., Checkel, J. L., and Gleich, G. J. (1992) Eosinophil-derived neurotoxin and human liver ribonuclease. *J. Biol. Chem.* **267**, 14859–14865.
10. Futami, J., Seno, M., Kosaka, M., Tada, H., Seno, S., and Yamada, H. (1995) Recombinant human pancreatic ribonuclease produced in *E. coli*: Importance of the amino-terminal sequence. *Biochem. Biophys. Res. Commun.* **216**, 406–413.
11. Rosenberg, H. F., and Dyer, K. D. (1995) Eosinophil cationic protein and eosinophil-derived neurotoxin. *J. Biol. Chem.* **270**, 21539–21544.
12. Shapiro, R., and Vallee, B. L. (1987) Human placental ribonuclease inhibitor abolishes both angiogenic and ribonucleolytic activities of angiogenin. *Proc. Natl. Acad. Sci. USA* **84**, 2238–2241.
13. Lee, F. S., Shapiro, R., and Vallee, B. L. (1989) Tight-binding inhibition of angiogenin and ribonuclease A by placental ribonuclease inhibitor. *Biochemistry* **28**, 225–230.
14. Vicentini, A. M., Kieffer, B., Mathies, R., Meyhack, B., Hemmings, B. A., Stone, S. R., and Hofsteenge, J. (1990) Protein chemical and kinetic characterization of recombinant porcine ribonuclease inhibitor expressed in *Saccharomyces cerevisiae*. *Biochemistry* **29**, 8827–8834.
15. Beintema, J. J., Schüller, C., Irie, M., and Carsana, A. (1988) Molecular evolution of the ribonuclease superfamily. *Prog. Biophys. Mol. Biol.* **51**, 165–192.
16. Lee, F. S., and Vallee, B. L. (1993) Structure and action of mammalian ribonuclease (angiogenin) inhibitor. *Prog. Nucleic Acid Res. Mol. Biol.* **44**, 1–30.
17. Riordan, J. F. (1997) in *Ribonucleases: Structures and Functions* (D'Alessio, G., and Riordan, J. F., Eds.), pp. 445–489, Academic Press, New York.
18. Strydom, D. J. (1998) The angiogenins. *Cell. Mol. Life Sci.* **54**, 811–824.
19. Badet, J. (1999) Angiogenin, a potent mediator of angiogenesis. *Pathol. Biol.* **47**, 345–351.
20. Leland, P. A., Schultz, L. W., Kim, B.-M., and Raines, R. T. (1998) Ribonuclease A variants with potent cytotoxic activity. *Proc. Natl. Acad. Sci. USA* **98**, 10407–10412.
21. Bretscher, L. E., Abel, R. L., and Raines, R. T. (2000) A ribonuclease A variant with low catalytic activity but potent cytotoxicity. *J. Biol. Chem.* **275**, 9893–9896.
22. Leland, P. A., Staniszewski, K. E., Kim, B.-M., and Raines, R. T. (2001) Endowing human pancreatic ribonuclease with toxicity for cancer cells. *J. Biol. Chem.* **276**, 43095–43102.
23. Leland, P. A., and Raines, R. T. (2001) Cancer chemotherapy—Ribonucleases to the rescue. *Chem. Biol.* **8**, 405–413.
24. Youle, R. J., and D'Alessio, G. (1997) in *Ribonucleases: Structures and Functions* (D'Alessio, G., and Riordan, J. F., Eds.), pp. 491–514, Academic Press, New York.
25. Boix, E., Wu, Y., Vasandani, V. M., Saxena, S. K., Ardelt, W., Ladner, J., and Youle, R. J. (1996) Role of the N terminus in RNase A homologues: Differences in catalytic activity, ribonuclease inhibitor interaction and cytotoxicity. *J. Mol. Biol.* **257**, 992–1007.
26. Lee, F. S., Auld, D. S., and Vallee, B. L. (1989) Tryptophan fluorescence as a probe of placental ribonuclease inhibitor binding of angiogenin. *Biochemistry* **28**, 219–224.
27. Klink, T. A., Vicentini, A. M., Hofsteenge, J., and Raines, R. T. (2001) High-level soluble production and characterization of porcine ribonuclease inhibitor. *Protein Expression Purif.* **22**, 174–179.
28. Ferreras, M., Gavilanes, J. G., López-Otín, C., and García-Segura, J. M. (1995) Thiol-disulfide exchange of ribonuclease inhibitor bound to ribonuclease A. *J. Biol. Chem.* **270**, 28570–28578.
29. Kothandaraman, S., Hebert, M. C., Raines, R. T., and Nibert, M. L. (1998) No role for pepstatin-A-sensitive acidic proteinase in reovirus infections of L or MDCK cells. *Virology* **251**, 264–272.
30. Sweeney, R. Y., Kelemen, B. R., Woycechowsky, K. J., and Raines, R. T. (2000) A highly active immobilized ribonuclease. *Anal. Biochem.* **286**, 312–314.
31. delCardayré, S. B., Ribó, M., Yokel, E. M., Quirk, D. J., Rutter, W. J., and Raines, R. T. (1995) Engineering ribonuclease A: Production, purification, and characterization of wild-type enzyme and mutants at Gln11. *Protein Eng.* **8**, 261–273.
32. Messmore, J. M., Fuchs, D. N., and Raines, R. T. (1995) Ribonuclease A: Revealing structure–function relationships with semi-synthesis. *J. Am. Chem. Soc.* **117**, 8057–8060.
33. Messmore, J. M., Holmgren, S. K., Grilley, J. E., and Raines, R. T. (2000) Sulfur shuffle: Modulating enzymatic activity by thiol–disulfide interchange. *Bioconjugate Chem.* **11**, 408–413.
34. Sela, M., Anfinsen, C. B., and Harrington, W. F. (1957) The correlation of ribonuclease activity with specific aspects of tertiary structure. *Biochim. Biophys. Acta* **26**, 502–512.
35. Leland, P. A., Staniszewski, K. E., Park, C., Kelemen, B. R., and Raines, R. T. (2002) The ribonucleolytic activity of angiogenin. *Biochemistry* **41**, 1343–1350.
36. Raines, R. T., Toscano, M. P., Nierengarten, D. M., Ha, J. H., and Auerbach, R. (1995) Replacing a surface loop endows ribonuclease A with angiogenic activity. *J. Biol. Chem.* **270**, 17180–17184.
37. Lin, S.-Y., and Riggs, A. D. (1972) *lac* repressor binding to non-operator DNA: Detailed studies and a comparison of equilibrium and rate competition methods. *J. Mol. Biol.* **72**, 671–690.
38. Chen, C.-Z., and Shapiro, R. (1997) Site-specific mutagenesis reveals differences in the structural bases for tight binding of RNase inhibitor to angiogenin and RNase A. *Proc. Natl. Acad. Sci. USA* **94**, 1761–1766.
39. Chen, C.-Z., and Shapiro, R. (1999) Superadditive and subadditive effects of “hot spot” mutations within the interfaces of placental ribonuclease inhibitor with angiogenin and ribonuclease A. *Biochemistry* **38**, 9273–9285.
40. Shapiro, R., Ruiz-Gutierrez, M., and Chen, C.-Z. (2000) Analysis of the interactions of human ribonuclease inhibitor with angiogenin and ribonuclease A by mutagenesis: Importance of inhibitor residues inside versus outside the C-terminal “hot spot.” *J. Mol. Biol.* **302**, 497–519.
41. Goldberg, J. M., and Baldwin, R. L. (1998) Kinetic mechanism of a partial folding reaction. 1. Properties of the reaction and effects of denaturants. *Biochemistry* **37**, 2546–2555.
42. Goldberg, J. M., and Baldwin, R. L. (1999) A specific transition state for S-peptide combining with folded S-protein and then refolding. *Proc. Natl. Acad. Sci. USA* **96**, 2019–2024.